Heliyon 10 (2024) e32686

Contents lists available at ScienceDirect

Heliyon

journal homepage: www.cell.com/heliyon

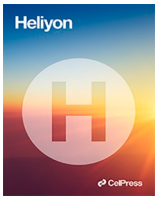

Research article

PSO/SDF-1 composite hydrogel promotes osteogenic differentiation of PDLSCs and bone regeneration in periodontitis rats

Wei Zhang [a], Minghong Liu [b], Di Wu [b], Yuanping Hao [b], Beibei Cong [b], Lihui Wang [a], Yujia Wang [a], Meihua Gao [b], Yingjie Xu [b,*], Yingtao Wu [b,**]

[a] School of Stomatology, Shandong Second Medical University, Weifang, 261053, China
[b] Qingdao Stomatological Hospital Affiliated to Qingdao University, Qingdao, 266001, China

ARTICLE INFO

Keywords:
Periodontitis
PSO
SDF-1
Hydrogel
Bone regeneration

ABSTRACT

Periodontitis is an inflammatory disease characterized by the destruction of periodontal tissues, and the promotion of bone tissue regeneration is the key to curing periodontitis. Psoralen is the main component of *Psoralea corylifolia* Linn, and has multiple biological effects, including anti-osteoporosis and osteogenesis. We constructed a novel hydrogel loaded with psoralen (PSO) and stromal cell-derived factor-1 (SDF-1) for direct endogenous cell homing. This study aimed to evaluate the synergistic effects of PSO/SDF-1 on periodontal bone regeneration in patients with periodontitis. The results of CCK8, alkaline phosphatase (ALP) activity assay, and Alizarin Red staining showed that PSO/SDF-1 combination treatment promoted cell proliferation, chemotaxis ability, and ALP activity of PDLSCs. qRT-PCR and western blotting showed that the expression levels of alkaline phosphatase (ALP), dwarf-associated transcription factor 2 (RUNX2), and osteocalcin (OCN) gene were upregulated. Rat periodontal models were established to observe the effect of local application of the composite hydrogel on bone regeneration. These results proved that the PSO/SDF-1 combination treatment significantly promoted new bone formation. The immunohistochemical (IHC) results confirmed the elevated expression of ALP, RUNX2, and OCN osteogenic genes. PSO/SDF-1 composite hydrogel can synergistically regulate the biological function and promote periodontal bone formation. Thus, this study provides a novel strategy for periodontal bone regeneration.

1. Introduction

Periodontitis is an inflammatory disease characterized by a destructive immune response and pathological bone resorption [1], which leads to gingival inflammation, periodontal pocket formation, alveolar bone resorption, and ultimately loosening and loss of teeth [2,3]. Restoring bone defects is the key to cure periodontitis [4]. Clinically, artificial bone powders is implanted to promote bone regeneration [5,6]. However, implantation takes a long time, bone grafting materials are expensive, and the recovery of artificial bone powder is not as good as bone tissue. Therefore, there is an urgent need to develop new methods for treating bone defects.

* Corresponding author.
** Corresponding author.
E-mail addresses: xyjdywe@163.com (Y. Xu), 347107303@qq.com (Y. Wu).

https://doi.org/10.1016/j.heliyon.2024.e32686
Received 20 February 2024; Received in revised form 5 June 2024; Accepted 6 June 2024
Available online 7 June 2024
2405-8440/© 2024 Published by Elsevier Ltd. This is an open access article under the CC BY-NC-ND license (http://creativecommons.org/licenses/by-nc-nd/4.0/).

The periodontium contributes to tooth homeostasis, nutrition, and repair of damaged tissues [7,8]. Recently, PDLSCs have been shown to promote the regeneration of periodontal tissues in patients with periodontitis [9–11]. PDLSCs may be an ideal material for periodontal tissue repair and regeneration. However, all PDLSC-based treatments require large numbers of PDLSCs, and obtaining sufficient PDLSCs is challeng [12]. Stromal cell-derived factor-1 (SDF-1), also known as the chemokine CXCL-12, is a small-molecule cytokine family protein that directs the migratory movements of stem cell, improving cell survival and promoting osteoblast proliferation [13–15]. Thus, it is a candidate for promoting *in situ* periodontal tissue regeneration. However, the application of SDF-1 alone is insufficient to promote bone regeneration [16], and the best way is to recruit endogenous stem cells *via* SDF-1 and promote the osteogenic differentiation of stem cells *via* other drugs [17].

Psoralen is a weak estrogen-like compound extracted from the leguminous plant *Psoralea corylifolia* Linn. It has multiple pharmacological activities, such as anti-osteoporosis [18–21]. Psoralen increases the expression of osteogenic markers and promotes osteoblast differentiation and bone regeneration [22,23]. Psoralen promotes the osteogenic differentiation of PDLSCs [24] and can be used as a potential periodontal bone tissue regeneration drug. Our previous studies demonstrated that the psoralen reduced expression levels of inflammatory factors and alveolar bone resorption [25].

Because of the unique oral environment, the topical application of psoralen ensures that higher concentrations in the epidermis compared to oral administration [26–28]. Gelatin Methacrylamide (GelMA) has received increasing attention because of its large number of functional groups, good biological properties, and many other advantages [29–32], and has been widely used in the fields of drug loading [33], biological tissue engineering [34], and bone defect repair [35,36], *etc*. Therefore, GelMA can be applied locally in oral cavity for drug release.

Therefore, this study aimed to construct a novel composite hydrogel based on the osteogenic properties of PSO and SDF-1, and study its regulatory effect on the osteogenic differentiation of periodontal membrane stem cells. This study provides a novel approach curing periodontitis.

2. Materials and methods

2.1. Cell culture

Patients aged 18–25 years (all signed an informed consent form) who required extraction of their premolars or third molars due to orthodontic reduction or obstruction were selected at the Qingdao Stomatological Hospital, and healthy teeth free of periodontal inflammation, caries, and dental defects were obtained. The periodontal membranes were extracted and cultured as periodontal membrane stem cells. This study was approved by the Ethics Committee of Qingdao Stomatological Hospital (2023KQYX011).

Periodontal membranes were scraped from 1/3 of the tooth root to culture PDLSCs, and the medium contained α-MEM (with different concentrations of fetal bovine serum according to experiments) (FBS, Procell, China, Wuhan) and 1 % penicillin-streptomycin (Israel Bioindustries). All cells were cultured at 37 °C under 5 % CO_2, and 3rd-6th generations PDLSCs were used in this study for subsequent experiments.

2.2. Cell identification

Flow cytometry was used to identify surface markers of PDLSCs. The 3rd generation PDLSCs with good cell activity were taken, and the cell density was adjusted to 1×10^4 cells/mL. The cell suspension was incubated with mouse anti-human antibodies CD34, CD45, CD73, and CD90 (Elabscience, Wuhan, China) (1:50) for 20 min at room temperature in the dark, and PBS was used as a control group. The expression levels of surface markers were analyzed by flow cytometry (DxFLEX, Beckman Coulter, Suzhou, China).

PDLSCs (2×10^5 cells/well) were inoculated in six-well plates and cultured in osteogenic differentiation induction medium (Procell, Wuhan, China) for 21 days, fixed with 4 % paraformaldehyde (Elabscience, Wuhan, China), stained with alizarin red, and observed under a light microscope.

PDLSCs (2×10^5 cells/well) were cultured in adipogenic differentiation induction medium (Procell, Wuhan, China) for 21 days. The cells were fixed with 4 % paraformaldehyde, stained with oil red O and observed under a light microscope.

3 mL of cell suspension with a cell density of 50 cells/mL PDLSCs was inoculated into Petri dishes and incubated at 37 °C in a 5 % CO_2 incubator. The solution was changed every 2–3 d until the formation of cellular colonies was visible under the microscope (size of 0.3–1 mm^2, clonogenic criteria $\geq$50 PDLSCs). After fixation, the cells were stained with 0.1 % crystal violet and photographed.

2.3. Selection of SDF-1 and PSO concentrations

To determine the optimal SDF-1 concentration (PeproTech, USA), PDLSCs (5×10^3 cells/well) were inoculated into 96-well plates, the original medium was discarded after 24 h, and complete medium containing different concentrations of SDF-1 (0, 10, 50, 100, 200, and 400 ng/mL) was added, with three replicate wells for each concentration. After culturing for 1, 2, and 3 days, cell proliferative capacity was determined using a CCK-8 kit (Absin Bioscience Inc., Shanghai, China). The absorbance was measured at 450 nm using a microplate reader (SynergyH1/H1M, Bio-Tek, China).

200 μL of PDLSCs (1×10^5 cells/well) cell suspension was added into the upper chamber of a 24-well Trans well migration plate, 700 μL of complete medium containing different concentrations of SDF-1 (0, 10, 50, 100, 200, 400 ng/mL) was added into the lower chamber. The cells that migrated through the membrane were fixed with 4 % paraformaldehyde, stained with 0.1 % crystal violet (Solarbio), then observed under the microscope, and the number of migrated cells was counted. All experiments were repeated three

times.

To determine the optimal PSO concentration, PDLSCs (5×10^3 cells/well) were inoculated in 96-well plates, and the original medium was discarded after 24 h. A complete culture medium containing different concentrations of PSO (0 μg/mL, 5 μg/mL, 10 μg/mL, 15 μg/mL, and 20 μg/mL dissolved in DMSO) (Solarbio, Beijing, China) was added for cell culture, with three replicate wells for each concentration. After 1, 3, 5, and 7 days of culture, the cell proliferative capacity was detected using kit 8. The absorbance was measured at 450 nm. Osteogenic differentiation ability at the optimal concentration was previously confirmed by our group.

200 μL of PDLSCs (1×10^5 cells/well) cell suspension was added into the upper chamber of a 24-well Trans well migration plate, 700 μL of complete medium containing different concentrations of PSO (0 μg/mL, 5 μg/mL, 10 μg/mL, 15 μg/mL, 20 μg/mL) was added to the lower chamber. The cells that migrated through the membrane were fixed with 4 % paraformaldehyde and stained with 0.1 % crystal violet to observe and count the cells; the experiment was repeated three times for each group.

2.4. Effect of PSO/SDF-1 on PDLSCs under gel-free conditions

PDLSCs (5×10^3 cells/well) were inoculated into 96-well plates, and the original medium was discarded after 24 h. The cells were divided into blank control, SDF-1, PSO, and PSO/SDF-1 groups and cultured in a complete medium, with three replicate wells for each group. After 1, 3, 5, and 7 d of culture, cell proliferation was detected using a counting kit 8. Absorbance was measured at 450 nm using a microplate reader.

Take a 24-well Transwell migration plate and add 200 μL of PDLSCs (1×10^5 cells/well) cell suspension into the upper chamber of each well, add 700 μL of complete medium containing different cell groupings (blank control group, SDF-1 group, PSO group and PSO/SDF-1 group) to the lower chamber, the cells migrated through the membrane were fixed with 4 % paraformaldehyde, and then stained with 0.1 % crystal violet to observe and count the cells, and the experiment was repeated three times in each group.

The P4 generation periodontal stem cells (2×10^5 cells/well) were inoculated in six-well plates cultured for 24 h. Next, they were added to the culture medium containing normal medium and SDF-1, PSO, and PSO/SDF-1, fixed with 4 % paraformaldehyde, stained with ALP staining work-up solution, and observed under a microscope. The results were quantitatively analyzed.

2.5. Synthesis and characterization of hydrogels

Dissolve 150 mg of GelMA with 3 mL of photoinitiator in a water bath at 65 °C avoiding light, mix 10 μg/mL PSO solution and 100 ng/mL SDF-1 solution with it, and then irradiate it with a 405 nm light source for 10 s to obtain PSO/SDF-1@GelMA material. PSO/SDF-1@GelMA is put into a 50 mL centrifuge tube with complete culture medium and is placed on a shaker (37 °C, 120 rpm) for 7 days. Then collect the extract, filter and remove bacteria, and placed in a new sterile centrifuge tube for 4 °C storage.

The surface morphology and pore size of the hydrogels were characterized using scanning electron microscopy (SEM); the swelling ratio (W_1–W_0/W_0) was calculated by measuring the mass of the lyophilized hydrogel (W_0) and the mass of the swelling hydrogel (W_1) in PBS at 37 °C for 4, 8, 12, 16, 20, 24, 28, 32, 36, 40, 44 and 48 h. All hydrogels were immersed in PBS buffer, then lyophilized and weighed every 5 days, and the degradation rate was calculated by recording the degradation weight of different hydrogels in PBS buffer; to assess the syringe ability of hydrogels, all light-cured hydrogels were injected into 1 mL syringes and squeezed, the continuity of the hydrogel and the gelling state were observed.

2.6. Retardation curves of SDF-1 and PSO in hydrogels

The hydrogel was shaken in PBS buffer at 37 °C for 6 h, 12 h, 24 h, 2 d, 4 d, 7 d, 10 d, and 15 d. The soak solutions were collected to determine the concentration of SDF-1 in the hydrogel using an SDF-1 enzyme immunoassay kit (ELISA, Elabscience, China). The results were replicated three times for each experimental group.

The hydrogel was shaken in PBS buffer at 37 °C for 1 d, 2 d, 3 d, 4 d, 5 d, 6 d, and 7 d. The soak solutions were collected to determine the PSO concentration using a UV spectrophotometer (at 246 nm), and the results were replicated three times for each experimental group.

2.7. Cytotoxicity and biocompatibility

PDLSCs were cultured in 96-well plates with maintenance medium for 24 h and replaced with medium containing different hydrogel extracts for 1, 3, 5, and 7 d. Cell proliferation was assayed using a CCK-8 kit, and the absorbance value was measured at 450 nm using a microplate reader.

2.8. In vitro chemotaxis and osteogenic differentiation

Different hydrogel extracts were added to a 24-well Transwell migration plate to detect the migration capacity, which was then stained with 0.1 % crystal violet, and the cells in the lower chamber were counted.

P4 generation periodontal stem cells (2×10^5 cells/well) were inoculated into six-well plates and cultured for 24 h. After incubation with different hydrogel extracts, all cells were fixed with 4 % paraformaldehyde, stained with ALP staining phosphatase, and observed under a microscope. After that, all cells were lysed on ice with RIPA (Elabscience, Wuhan, China). Proteins from different groups were extracted, the concentration was determined using a BCA kit (Elabscience, Wuhan, China), and ALP activity was calculated using an

ALP activity assay kit (Elabscience, Wuhan, China).

P4 generation periodontal membrane stem cells were inoculated in six-well plates. After incubation with different groups of hydrogel extracts, all cells were fixed with 4 % paraformaldehyde, stained with Alizarin Red, and observed under a light microscope. A cetylpyridinium chloride (CPC, Solarbio) solution was added to dissolve the calcium nodules, and the absorbance was measured at 562 nm.

2.9. RT-PCR and western blot detection

Human PDLSCs were inoculated in six-well plates at a density of 5×10^4/mL for 7 days with different groups of hydrogel extracts as described above. Total RNA was extracted, cDNA was reverse transcribed, and PCR amplification was performed to detect ALP, RUNX2, and OCN gene expression levels. The primers used were as following: ALP: ACT CTC CGA GAT GGT GGT GGT GGT GGT G (forward) and CGT GGT CAA TTC TGC CTC CTT CC (reverse); RUNX2: AGG CAG TTC CCA AGC ATT TCA TCC (forward) and TGG CAG GTA GGT GTG GTA GTG AG (reverse); OCN: AGG GCA GCG AGG TAG TGA AGA G (forward) and GGT CAG CCA ACT CGT CAC AGT C (reverse).

The total protein of each group was extracted by RIPA lysate, and the concentration of proteins was determined using a BCA kit. The proteins were separated by SDS-PAGE electrophoresis, then electrotransferred to PVDF membranes, and incubated with ALP (ab307726, Abcam), OCN (ab133612, Abcam), and RUNX2 (D1L7F, Cell Signaling) primary antibody (1:5000) at 4 °C overnight, the enzyme-labelled protein bands were exposed with ECL kit and photographed. The relative protein expression levels were analyzed using Image J 2.0 software with β-actin as an internal reference.

2.10. In vivo experiments

72 specific pathogen-free (SPF) SD male rats (Quality Certificate No. 370726230100935043, provided by Jinan Pangyue Laboratory Animal Breeding Co., Ltd.), which were 8 weeks old, were selected and randomly divided into 6 groups: normal group (healthy rats with no treatment), model group (periodontitis rats with no treatment), GelMA group (periodontitis rats treated with GelMA blank hydrogel), SDF-1@GelMA group (periodontitis rats treated with hydrogel containing SDF-1), PSO@GelMA group (periodontitis rats treated with hydrogel containing PSO), and PSO/SDF-1@GelMA group (periodontitis rats treated with composite hydrogel containing PSO and SDF-1). After anesthetization with pentobarbital sodium (40 mg/kg body weight), a standard ligating wire (0.25 mm) was wrapped and fixed around the maxillary first molar of the Wistar rats for 4 weeks. Finally, the gingiva of the first molar turned red and bled upon probing, had a deep periodontal pocket and alveolar bone resorption, and the teeth were slightly loosened. All the above results proved that the periodontitis model was successfully established.

In the GelMA group, SDF-1@GelMA group, PSO@GelMA group, and PSO/SDF-1@GelMA group, corresponding hydrogels were injected into the periodontal pockets on the midpoints of buccal and palatal aspects of maxillary first molars with a 1 mL syringe. The model group was injected with equal amounts of PBS at the same site, and no administration was administered to the normal group. All rats were sacrificed 4 weeks after hydrogel injection.

2.11. Micro-computed tomography (Micro-CT) analysis

Bone remodeling was analyzed (90 kV, 88 μA) using a Micro-CT (Qingdao University). The vertical distance between the cementoenamel junction (CEJ) and alveolar bone crest (AB), shown as CEJ-AB, was measured to indicate the degree of alveolar bone loss.

2.12. Histological analysis

Sections were decalcified with 10 % ethylenediaminetetraacetate (EDTA, Solarbio), dehydrated with a series of graded ethanol solutions, embedded in paraffin, and transverse sections (5 μm thick) of the first molar were cut along the proximal-distal-medial direction. The prepared sections were stained with hematoxylin and eosin (H&E, Solarbio) and photographed to analyze periodontal tissue morphology.

2.13. Immunohistochemical (IHC) staining

Rabbit anti-ALP antibody (1:100, 18176-1-AP, Proteintech), RUNX2 (1:100, ab236639, Abcam), and OCN (1:100, 23418-1-AP, Proteintech) were used to incubated on sections overnight at 4 °C. Goat anti-rabbit IgG was used as a secondary antibody. Immunoreactivity was detected using a 3,3 ' - diaminobenzidine (DAB, Solarbio) solution. Cell nuclei were stained with hematoxylin and mounted. Images were captured using a microscope. Image Pro Plus software (version 6.0) was used to measure integrated optical density (IOD).

2.14. Statistical analyses

All data were expressed as mean ± SD. A *t*-test was used to compare the mean values between the two groups. In addition, the results of the statistical analysis showed that each data group had a normal distribution. Therefore, we used a one-way ANOVA to

compare the mean values among the arrows. Statistical analyses were performed using Graph Pad Prism 9 software (*, $P < 0.05$; **, $P < 0.01$; ***, $P < 0.001$; ****, $P < 0.0001$; #, $P < 0.05$; ##, $P < 0.01$; ###, $P < 0.001$; ####, $P < 0.0001$).

3. Results

3.1. Identification of periodontal ligament stem cells (PDLSCs)

Results showed primary cultures of single-cell suspensions, P1, P2, and P3 generations of PDLSCs were all typically long fusiform (Fig. 1A: a, b, c, and d). The flow cytometry analysis showed significant expression of CD73 on the surface of PDLSCs at 99.44 % and CD90 at 99.8 %. In contrast, the antibodies CD34 and CD45 showed low expression (Fig. 1B). Fig. 1C showed that the cells possessed osteogenic and lipogenic features, and mineralized nodules and lipid droplets were observed. Colony experiments showed that PDLSCs could form a single colony after culture in low density. The results indicated that the PDLSCs met the basic standards for MSCs and were identified as periodontal membrane stem cells [37], which could be used for subsequent experiments.

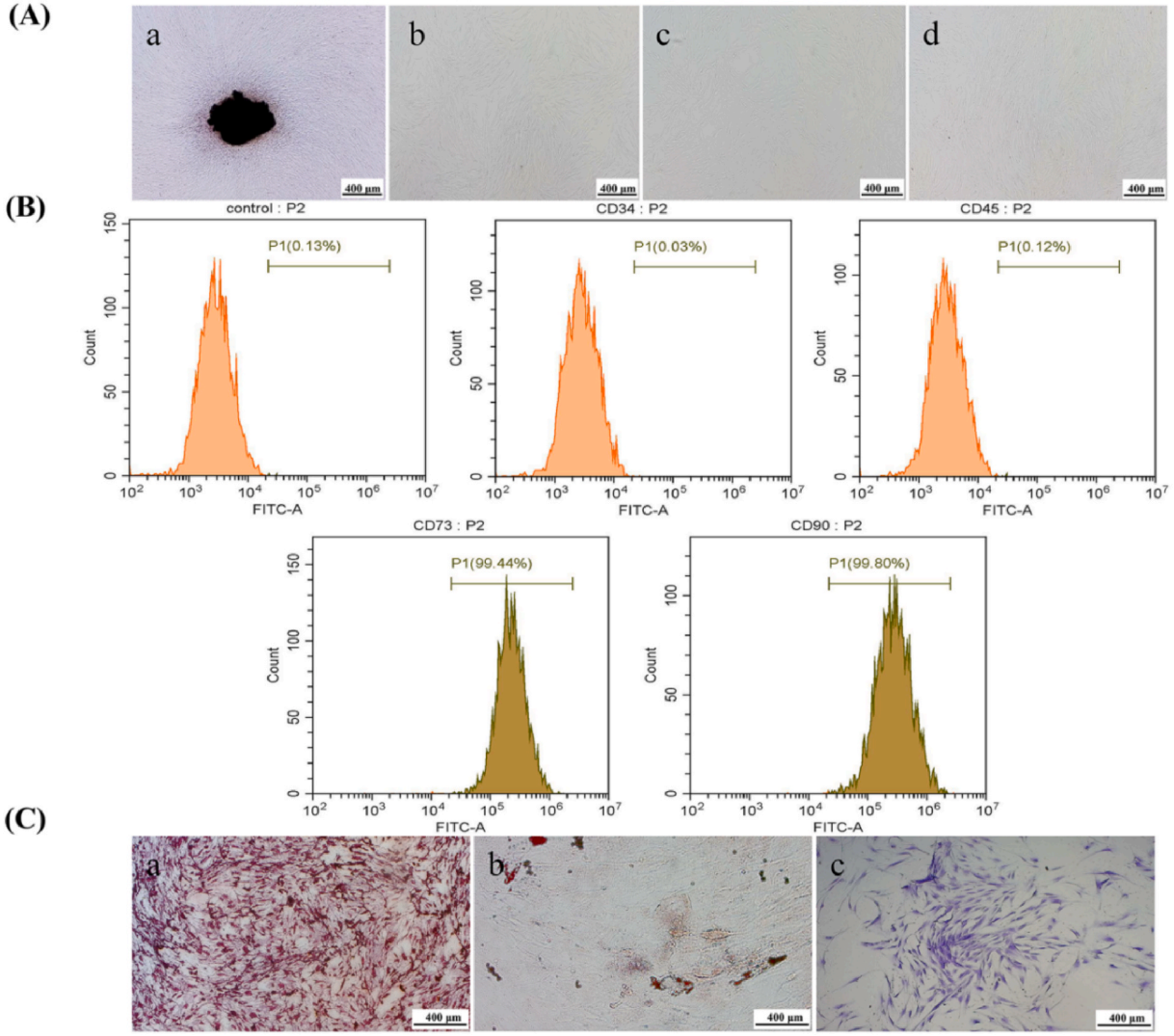

Fig. 1. Identification of PDLSCs. (A) a: the morphology of periodontal tissue and primary PDLSCs; b: the morphology of P1; c: the morphology of P2; d: the morphology of P3. (B) Identification of surface antibodies to PDLSCs. (C) a: a representative picture of osteogenic differentiation of PDLSCs; b: a representative picture of lipogenic differentiation of PDLSCs; c: clusters of cells originating from PDLSCs forming single colonies. The scale bar is 400 μm.

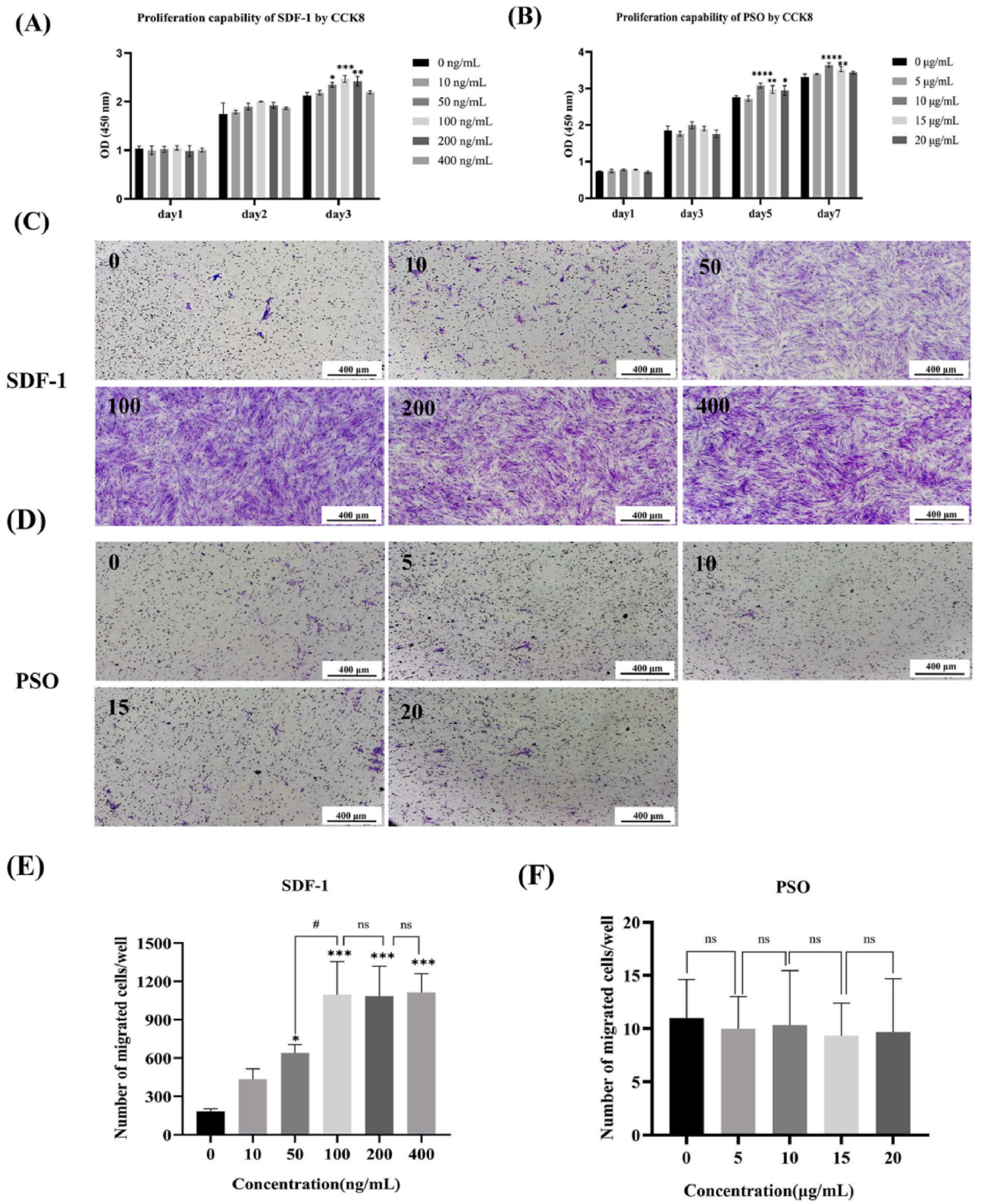

(caption on next page)

Fig. 2. Determination of SDF-1 and PSO concentrations. (A) Effects of different concentrations of SDF-1 on proliferation capacity of PDLSCs (ng/mL) by CCK8. *, $P < 0.05$; **, $P < 0.01$; ***, $P < 0.001$; ****, $P < 0.0001$ *vs* 0 ng/mL group. (B) Effects of different concentrations of PSO on proliferation capacity of PDLSCs (μg/mL) by CCK8. *, $P < 0.05$; **, $P < 0.01$; ***, $P < 0.001$; ****, $P < 0.0001$ *vs* 0 μg/mL group. (C) Representative pictures of the migration ability of PDLSCs at different concentrations of SDF-1 (ng/mL). (D) Representative pictures of the migration ability of PDLSCs at different concentrations of PSO (μg/mL). (E) Quantitative analysis of cell migration at different concentrations of SDF-1. *, $P < 0.05$; **, $P < 0.01$; ***, $P < 0.001$; ****, $P < 0.0001$ *vs* 0 ng/mL group. #, $P < 0.05$ *vs* 50 ng/mL group, ns: no significant difference. (F) Quantitative analysis of cell migration at different concentrations of PSO. ns: no significant difference. Data are expressed as mean ± SD, N = 3. The scale bar is 400 μm.

3.2. Determination of SDF-1 and PSO concentrations

CCK8 results showed that 100 ng/mL SDF-1 and 10 μg/mL of PSO could promote the PDLSCs to proliferate most strongly ($P < 0.001$) (Fig. 2A and B). Then, the results of the transwell migration assay showed that, at 0–100 ng/mL, the recruiting ability of SDF-1 to PDLSCs increased gradually depending on concentration ($P < 0.001$); when the concentration was more than 100 ng/mL, the number of cells was no longer increased, and there was no statistically significant difference between the two groups (Fig. 2C and E). In contrast, the recruiting ability of PSO to PDLSCs did not increase significantly ($P > 0.05$) (Fig. 2D and F). Furthermore, the effect of 10 μg/mL PSO on the osteogenic ability of PDLSCs has been demonstrated by our previous research [38]. Therefore, this study determined that the optimal concentration of SDF-1 was 100 ng/mL, and the optimal concentration of PSO was 10 μg/mL.

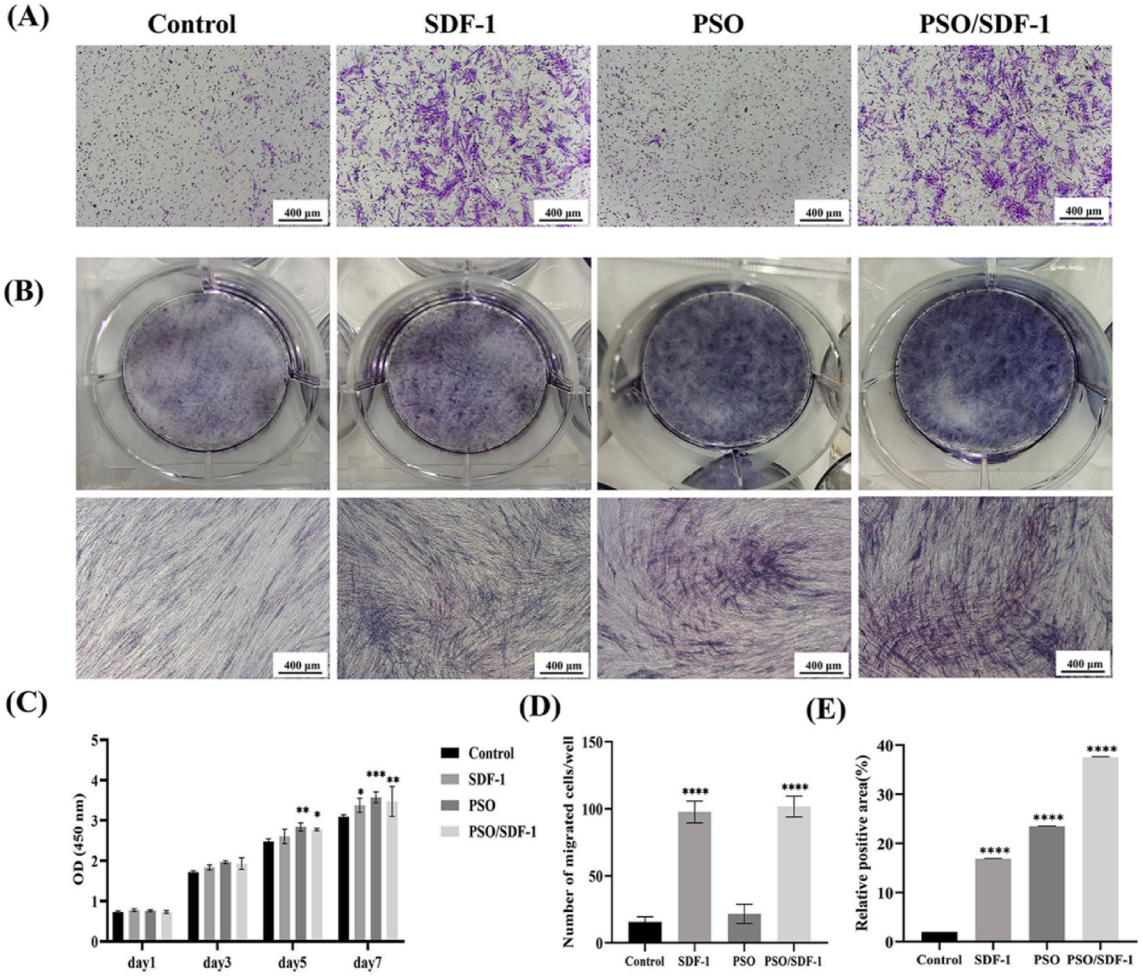

Fig. 3. The effect of PSO and SDF-1 combined application in gel-free condition on PDLSCs. (A) Representative pictures of the migration ability of PDLSCs in different groups. (B) Representative pictures of ALP staining in different groups. (C) Effects of different groups on proliferation capacity of PDLSCs. (D) Quantitative analysis of cell migration. (E) Quantitative analysis of ALP staining. Data are expressed as mean ± SD, N = 3. *, $P < 0.05$; **, $P < 0.01$; ***, $P < 0.001$; ****, $P < 0.0001$ *vs* Control group. The scale bar is 400 μm.

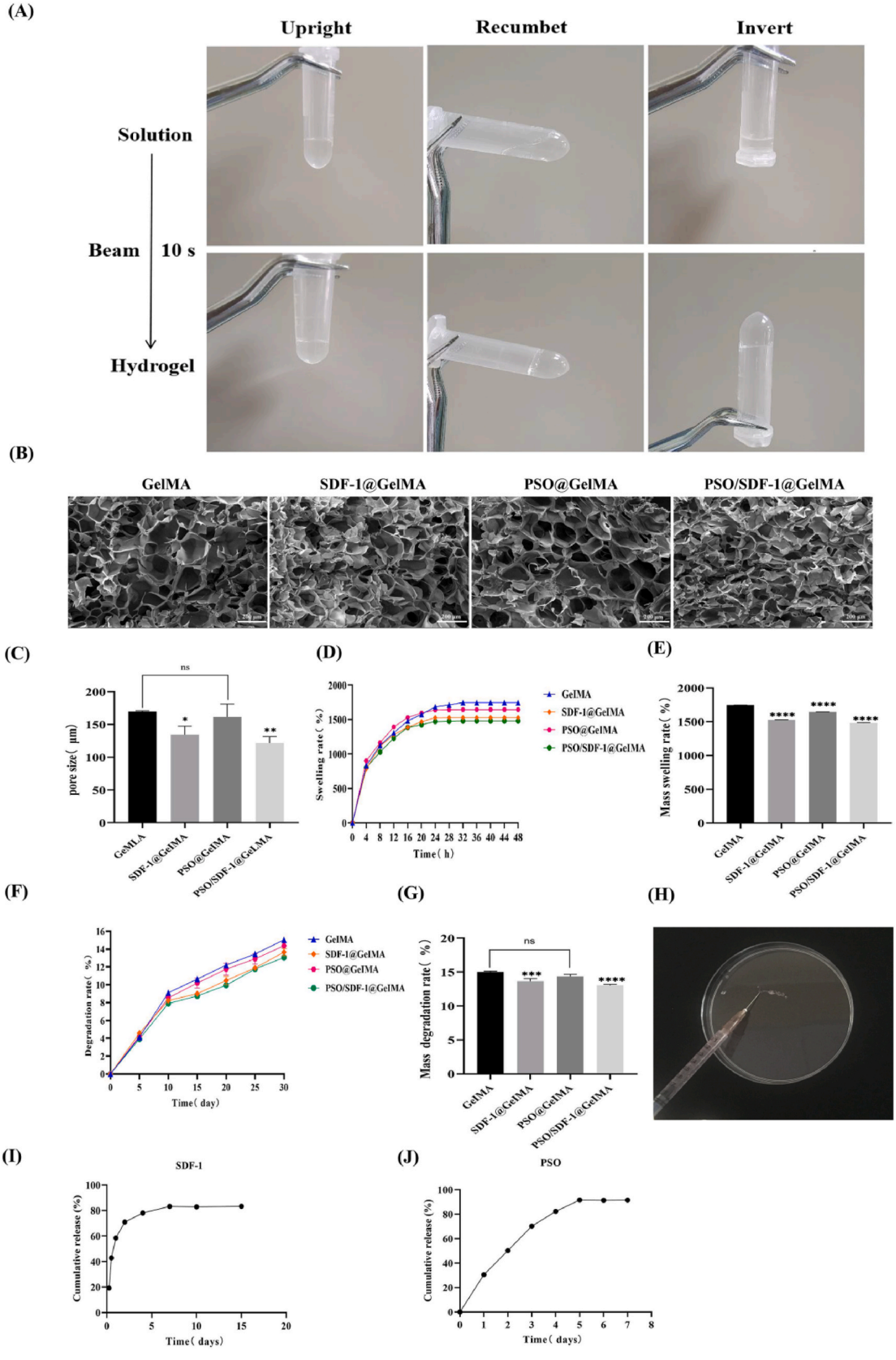

(caption on next page)

Fig. 4. Preparation and characterization of the hydrogels. (A) Representative photograph of hydrogel after light. (B) SEM images of the hydrogels. The scale bar is 200 μm. (C) The mean pore size of the hydrogels. (D) Dissolution curve of the hydrogels. (E) Quantitative dissolution analysis of the hydrogels. (F) Degradation curve of the hydrogels. (G) Quantitative degradation analysis of the hydrogels. (H) Injectability and continuity of the hydrogels. (I) SDF-1 retardation curves. (J) PSO retardation curves. Data are expressed as mean ± SD, N = 3. *, $P < 0.05$; **, $P < 0.01$; ***, $P < 0.001$; ****, $P < 0.0001$ *vs* GelMA group, ns: no significant difference.

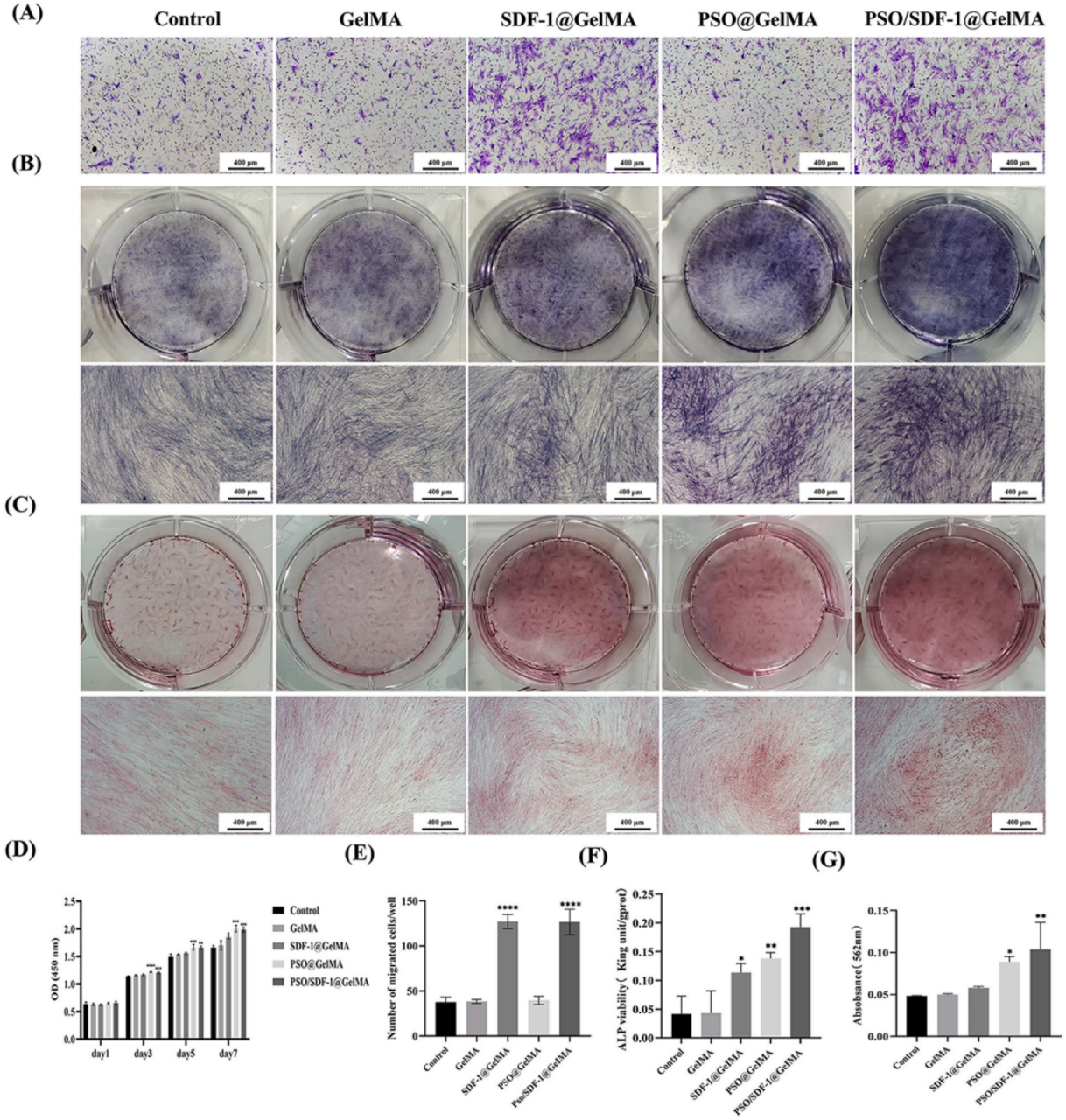

Fig. 5. Effects of different hydrogels on PDLSCs. (A) Representative pictures of the migration ability of PDLSCs. (B) Representative pictures of ALP staining. (C) Representative pictures of alizarin red staining. (D) Effects of different hydrogels on proliferation capacity of PDLSCs. (E) Quantitative analysis of cell migration. (F) Quantitative analysis of ALP staining. (G) Quantitative analysis of Alizarin red staining. Data are expressed as mean ± SD, N = 3. *, $P < 0.05$; **, $P < 0.01$; ***, $P < 0.001$; ****, $P < 0.0001$ *vs* Control group. The scale bar is 400 μm. (For interpretation of the references to color in this figure legend, the reader is referred to the Web version of this article.)

3.3. The combined action of PSO and SDF-1 in gel-free conditions improved the proliferation and osteogenic differentiation ability of PDLSC

The CCK8 results showed that compared with the control group, the combined application of PSO/SDF-1 significantly promoted PDLSCs proliferation ($P < 0.05$) (Fig. 3C). In addition, the Transwell migration assay showed that the number of migrated cells was significantly increased in the SDF-1 and PSO/SDF-1 groups compared with the control group. The difference in cell numbers was statistically significant ($P < 0.0001$). This indicated that the combined application of SDF-1 and PSO did not affect the recruitment and proliferative ability of SDF-1 in PDLSCs (Fig. 3A and D).

ALP staining showed that compared with the control group, the SDF-1, PSO, and PSO/SDF-1 groups all showed a blue-black color, indicating that ALP was produced in the three groups. Quantitative results showed that the expression levels of ALP were gradually enhanced, and compared with the other groups, the positive area of PSO/SDF-1 was the largest, indicating that PSO/SDF-1 had the strongest osteogenic differentiation ability (Fig. 3B and E).

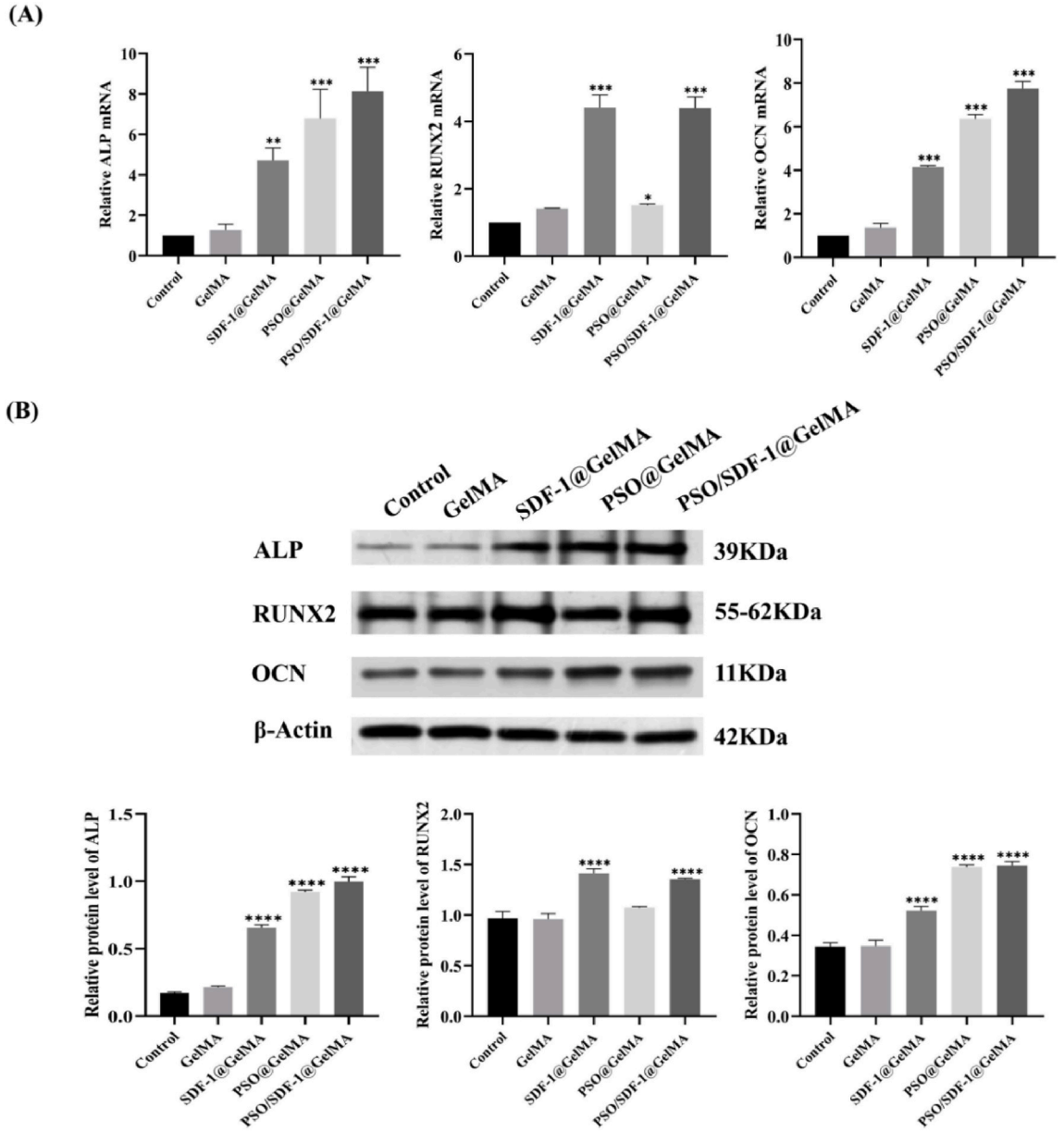

Fig. 6. Expression of osteogenic genes of PDLSCs by the hydrogels. (A) The mRNA expression level of ALP, RUNX2 and OCN. (B) The protein expression level of ALP, RUNX2, and OCN. Data are expressed as mean ± SD, N = 3. *, $P < 0.05$; **, $P < 0.01$; ***, $P < 0.001$; ****, $P < 0.0001$ *vs* Control group.

3.4. Physical characteristics of hydrogels

As shown in Fig. 4A, hydrogels were successfully synthesized in 10 s under 405 nm irradiation, according to the above method. Scanning electron microscopy revealed that all four hydrogels had loose porous structures with different pore sizes and uniform distributions. Compared to GelMA, the average pore size of PSO@GelMA did not change much, and the average pore size of SDF-1@GelMA and PSO/SDF-1@GeLMA decreased slightly ($P < 0.05$) (Fig. 4B and C); GelMA, SDF-1@GelMA, PSO@GelMA and PSO/SDF-1@GelMA all showed faster dissolution rate in the first 8 h, compared to GelMA, the dissolution rate of SDF-1@GelMA, PSO@GelMA and PSO/SDF-1@GelMA is reduced ($P < 0.0001$) (Fig. 4D and E). Degradation experiments showed that GelMA, SDF-1@GelMA, PSO@GelMA, and PSO/SDF-1@GelMA degraded faster in the first 10 days, and PSO/SDF-1@GelMA had the lowest degradation rate compared to that of GelMA ($P < 0.0001$) (Fig. 4F and G). The light-cured PSO/SDF-1@GelMA passed through a 1 mL syringe needle freely and continuously (Fig. 4H). These results confirm that the hydrogel is injectable. The slow-release experiment showed that the early release of SDF-1 was fast and concentrated, reaching equilibrium in 7 days (Fig. 4I). In contrast, PSO was released slowly and steadily, reaching equilibrium after 5 days (Fig. 4J).

3.5. Effect of multiple composite hydrogels on PDLSCs

The CCK8 results showed that, compared with the control group, the PSO/SDF-1@GelMA group significantly promoted cell proliferation ($P < 0.05$) (Fig. 5D). The transwell migration assay showed that SDF-1@GelMA and PSO/SDF-1@GelMA significantly enhanced the migration of PDLSCs compared to the control group. The difference was statistically significant ($P < 0.0001$), suggesting that the hydrogel did not affect the effect of PSO/SDF-1 on cells (Fig. 5A and E).

The ALP staining showed that the SDF-1@GelMA, PSO@GelMA and PSO/SDF-1@GelMA groups were all blue-black. The results of ALP activity test showed that the expression levels of ALP were gradually enhanced in the SDF-1@GelMA, PSO@GelMA, and PSO/SDF-1@GelMA groups compared to the control group ($P < 0.05$) (Fig. 5B and F). Calcium nodules were observed in SDF-1@GelMA, PSO@GelMA and PSO/SDF-1@GelMA groups, and the quantitative analysis results showed the same trend that of ALP ($P < 0.05$) (Fig. 5C and G), indicating that PSO/SDF-1@GelMA had the strongest ability to promote osteogenic differentiation of PDLSCs.

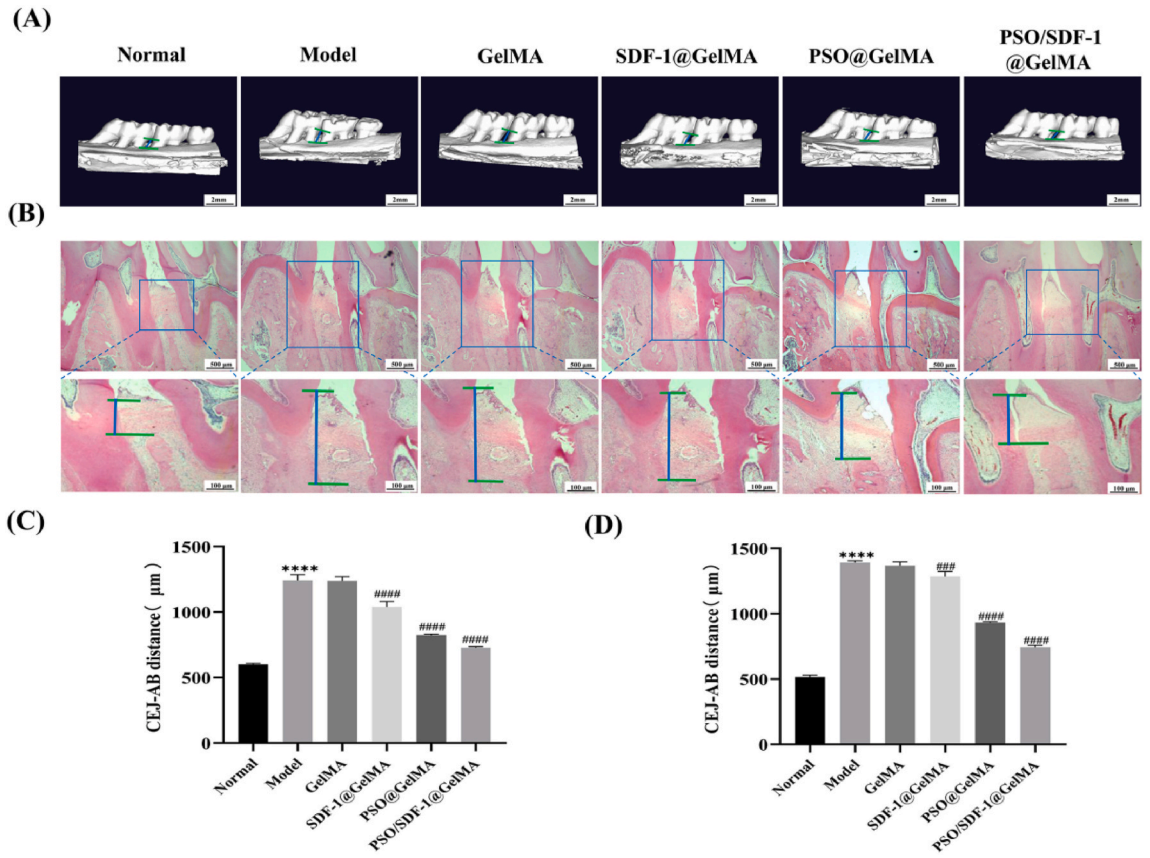

Fig. 7. The effect of PSO/SDF-1@GelMA on periodontal bone regeneration in situ. (A) Micro-CT 3D reconstruction. The scale bar is 2 mm. (B) Representative pictures of HE staining. The scale bar is 500 μm and 100 μm. (C) Quantitative analysis of Micro-CT. (D) Quantitative analysis of HE staining. Data are expressed as mean ± SD, N = 6. ****, $P < 0.0001$ *vs* Normal group; ###, $P < 0.001$; ####, $P < 0.0001$ *vs* Model group.

3.6. PSO/SDF-1@GelMA promoted the expression of osteogenic genes in PDLSCs

RT-PCR experiments showed that compared with the control group, the mRNA expressions of ALP and OCN were gradually higher in the SDF-1@GelMA group, PSO@GelMA group and PSO/SDF-1@GelMA group ($P < 0.001$); compared with the control group, the mRNA expression level of RUNX2 in the PSO/SDF-1@GelMA group was increased significantly ($P < 0.001$) (Fig. 6A). Western blot results showed that the protein expressions of ALP and OCN in SDF-1@GelMA group, PSO@GelMA group and PSO/SDF-1@GelMA group were gradually increased ($P < 0.001$); compared with the control group, RUNX2 protein expression level in PSO/SDF-

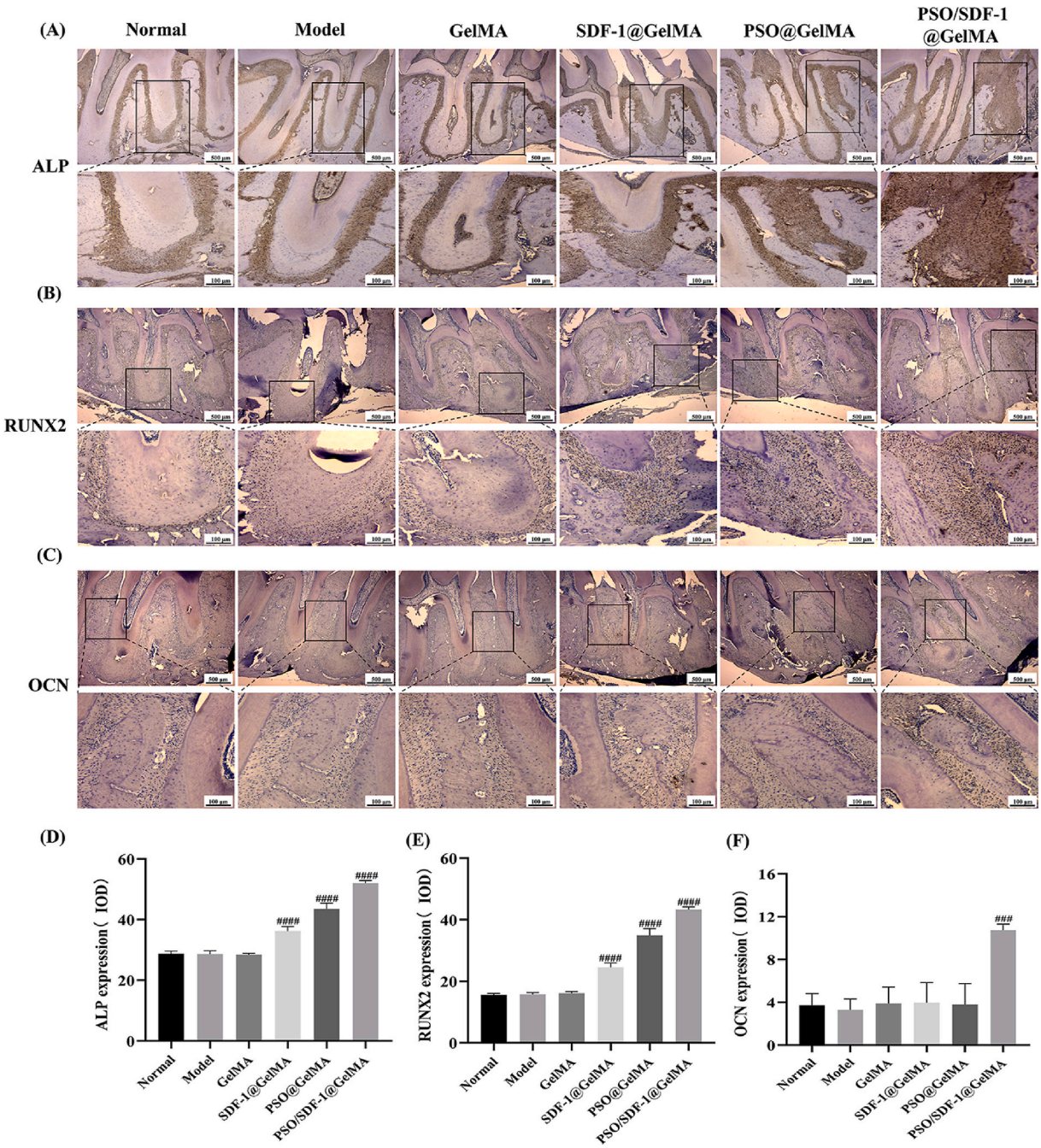

Fig. 8. IHC analysis of different hydrogels. (A) Representative pictures of IHC of ALP. The scale bar is 500 μm and 100 μm. (B) Representative pictures of IHC of RUNX2. The scale bar is 500 μm and 100 μm. (C) Representative pictures of IHC of OCN. The scale bar is 500 μm and 100 μm. (D) IHC quantitative analysis of ALP. (E) IHC quantitative analysis of RUNX2. (F) IHC quantitative analysis of OCN. Data are expressed as mean ± SD, N = 6. ###, $P < 0.001$; ####, $P < 0.0001$ *vs* Model group.

1@GelMA group was significantly increased ($P < 0.001$), which showed the same trend as RT-PCR (Fig. 6B). The above results showed that, PSO/SDF-1@GelMA can promote the mRNA and protein expression levels of ALP, RUNX2 and OCN.

3.7. PSO/SDF-1@GelMA hydrogel promoted periodontal bone regeneration in periodontitis rats

The micro-CT and HE staining results showed that the alveolar bone of the model group exhibited vertical bone absorption, and the CEJ−AB distance increased by > 1.1 times compared with the normal group, which indicated that the periodontitis model had been successfully established ($P < 0.0001$). The CEJ-AB distance of the PSO/SDF-1@GelMA group was significantly smaller than that of the model group after four weeks of continuous injection ($P < 0.0001$) (Fig. 7A and C). H&E staining further confirmed that the degree of bone absorption in the PSO/SDF-1@GelMA group was significantly lower than that in the model group ($P < 0.0001$) (Fig. 7B and D). Therefore, the PSO/SDF-1@GelMA hydrogel significantly promoted alveolar bone regeneration.

3.8. PSO/SDF-1@GelMA significantly increased the expression level of the osteogenic genes in periodontitis rats

The IHC results showed that compared with the model group, the expression levels of ALP gradually increased in the SDF-1@GelMA, PSO@GelMA, and PSO/SDF-1@GelMA groups ($P < 0.0001$) (Fig. 8A and D), and the expression of RUNX2 and ALP showed the same trend (Fig. 8B and E).

There was no significant difference in the expression of OCN in the SDF-1@GelMA and PSO@GelMA groups compared to that in the model group ($P > 0.05$); however, there was a statistically significant difference in the PSO/SDF-1@GelMA group ($P < 0.001$) (Fig. 8C and F). Therefore, the PSO/SDF-1@GelMA significantly promoted the expression of ALP, RUNX2, and OCN.

4. Discussion

Periodontitis can lead to alveolar bone absorption, tooth loosening, and tooth loss; thus, promoting periodontal bone regeneration is crucial. In this study, PSO, which is known to promote osteogenic differentiation of cells, was co-loaded onto GelMA with SDF-1 (PSO/SDF-1@GelMA), a potent stromal cell-homing factor, to evaluate the effect of the composite hydrogel on periodontal bone regeneration. We demonstrated that the PSO/SDF-1@GelMA enhanced the proliferation, chemotaxis, and osteogenic differentiation of PDLSCs *in vitro*. Second, the local application of PSO/SDF-1@GelMA *in vivo* significantly promoted periodontal bone regeneration in rats with periodontitis.

It has been demonstrated that PDLSCs can promote periodontal tissue regeneration and thus have the potential to treat periodontitis. This study successfully isolate and characterize PDLSCs. Furthermore, we demonstrate that PDLSCs have osteogenic and lipogenic differentiation potentials and significant colony-forming ability (Fig. 1A and C). The surface antibody assays proved that PDLSCs had the characteristics of MSCs (Fig. 1B), suggesting that they can be used as a cell model to study the osteogenic differentiation capacity. However, all PDLSC-based treatments require large amounts of PDLSCs, and we need to explore new ways to recruit enough PDLSCs; therefore, SDF-1, which has a remarkable ability to recruit cells, was adopted in this experiment. To further verify the recruitment ability of SDF-1 on PDLSCs, we investigated the effect of SDF-1 on PDLSCs through CCK8 and migration experiments and found that the effect of SDF-1 was dose-dependent and could recruit a large number of PDLSCs at a concentration of 0–400 ng/mL, and the 100 ng/mL of SDF-1 had the strongest recruitment ability (Fig. 2A–C, and E).

Psoralen, the main component of *Psoralea corylifolia* Linn, promotes bone tissue regeneration. Our group has confirmed that psoralen promotes alveolar bone regeneration in rats with periodontitis by affecting the intestinal barrier [25]; however, the bone regeneration effect of psoralen applied locally has not been confirmed. First, we investigated the effect of PSO on PDLSCs in the CCK8 and migration experiments. The results showed that PSO proliferated on PDLSCs at the concentration of 0–20 μg/mL, but the 10 μg/mL of PSO had the strongest proliferation ability (Fig. 2B–D, and F). Therefore, this study determined 10 μg/mL of PSO and 100 ng/mL of SDF-1 as the optimal concentrations of PDLSCs.

Few studies have investigated the synergistic effects of PSO and SDF-1 on PDLSCs. Therefore, this study applied the combination of PSO and SDF-1 (PSO/SDF-1) to investigate its effect on the osteogenic differentiation of PDLSCs. The results showed that PSO/SDF-1 had a better effect on the osteogenic differentiation of PDLSCs than that of PSO and SDF-1 alone (Fig. 3). Therefore, in this study, PSO/SDF-1 was used as a potential therapeutic agent to promote periodontal bone tissue regeneration.

However, the oral environment is complex, and therapeutic drugs are easily diluted, making it difficult to preserve their effective concentrations. GelMA is safe, non-toxic, and widely applied in various fields. In this experiment, PSO, SDF-1, and PSO/SDF-1 were loaded onto the GelMA (PSO@GelMA, SDF-1@GelMA, and PSO/SDF-1@GelMA) respectively (Fig. 4A). Physical characterization showed that the hydrogels were injectable and could be used for periodontal pocket injections (Fig. 4H). The pore size of PSO/SDF-1@GelMA was smaller than that of the other groups, which proved that PSO and SDF-1 were loaded on GelMA at the same time (Fig. 4B and C). The curve of dissolution degradation and slow-release experiments proved that PSO/SDF-1@GelMA had high tissue affinity (Fig. 4D, E, F, and G) and excellent slow-release properties (Fig. 4I and J).

To determine whether the drug-loaded hydrogel reduced the effect of PSO/SDF-1 on PDLSCs, we simulated the release state of hydrogel injected into the periodontal pocket, The hydrogels were placed in the medium, so PSO and SDF-1 could be released from the hydrogels into the medium. Then we used the medium containing PSO and SDF-1 to culture the cells of all groups, and detected the effect of PSO and SDF-1 on PDLSCs by CCK8, ALP, and Alizarin Red staining. The results showed that PSO and SDF-1 promoted the proliferation and osteogenic differentiation of PDLSCs, while PSO/SDF-1@GelMA improved strongestly (Fig. 5). Therefore, the hydrogels did not influence the effect of PSO/SDF-1. To clarify the mechanism of osteogenic differentiation, we measured the

expression levels of osteogenic genes. ALP is a vital osteoblast differentiation biomarker that correlates with bone height [39]. RUNX2 is a key transcription factor involved in osteoblast differentiation and can bind to osteoblast-specific *cis*-acting elements to turn on the expression of bone matrix remodeling genes, thereby promoting bone formation [40]. OCN is a late marker of osteoblast differentiation, and its expression level is considered an essential indicator for evaluating cell differentiation into osteoblasts [41]. Therefore, we investigated the expression of ALP, RUNX2, and OCN. We concluded that the hydrogels loaded with drugs increased the mRNA and protein expression levels of ALP, RUNX2, and OCN (Fig. 6).

It was confirmed that PSO/SDF-1@GelMA had a noticeable effect on the PDLSCs *in vitro*. Next, the PSO/SDF-1@GelMA was injected into the periodontal pockets of rats with periodontitis to investigate the repair effects of PSO/SDF-1@GelMA on periodontitis rats. In the supplementary materials, it was proved that the PSO/SDF-1@GelMA had no toxic effect on the heart, liver, spleen, lung and kidney of periodontitis rats, which proved that it had biological compatibility (Fig. S1). Micro-CT and HE staining results showed that the drug-loaded hydrogels promoted alveolar bone regeneration in rats with periodontitis, in which PSO/SDF-1@GelMA had the most significant effect (Fig. 7). Whether the hydrogel loaded with drugs can also promote alveolar bone regeneration in animals by osteogenic genes, we further clarified by IHC, and the results showed that PSO/SDF-1@GelMA significantly increased the protein expression levels of ALP, RUNX2 and OCN (Fig. 8).

5. Conclusion

In summary, the combined application of PSO and SDF-1 promotes the osteogenic differentiation of PDLSCs. The hydrogels loaded with PSO and SDF-1 exhibited good injectability, biocompatibility, slow-release performance, recruitment, and osteogenic differentiation abilities. The injection of PSO/SDF-1@GelMA into the periodontal pocket of rats with periodontitis effectively promoted alveolar bone regeneration and increased the expression of osteogenic genes. This study provides a theoretical basis to develop novel materials for treating periodontitis promoting periodontal tissue and bone regeneration.

Ethics statement

The animal study was approved by the Ethics Committee of Qingdao Stomatological Hospital (Ethics number: 2023KQYX011).

Data availability statement

Most of the data are available in all Figures of the manuscripts. Moreover, the data will available on request.

CRediT authorship contribution statement

Wei Zhang: Writing – original draft, Visualization, Software, Methodology, Investigation, Formal analysis. **Minghong Liu:** Resources, Investigation. **Di Wu:** Resources, Investigation. **Yuanping Hao:** Resources, Investigation. **Beibei Cong:** Methodology, Investigation. **Lihui Wang:** Investigation. **Yujia Wang:** Investigation. **Meihua Gao:** Investigation. **Yingjie Xu:** Writing – review & editing, Validation, Supervision, Funding acquisition, Conceptualization. **Yingtao Wu:** Supervision, Resources, Funding acquisition.

Declaration of competing interest

The authors declare that they have no known competing financial interests or personal relationships that could have appeared to influence the work reported in this paper.

Acknowledgments

This work was supported by the National Natural Science Foundation of China (82301083), Shandong Provincial Natural Science Foundation (ZR2021MH388), Qingdao Traditional Chinese Medicine Research Program 2018–2019 (2019-zyy050), Chinese Medicine Science and Technology Project of Shandong Province (2021Z030), Qingdao Key Health Discipline Development Fund (2022–2024), Qingdao Clinical Research Center for Oral Diseases (22-3-7-lczx-7-nsh) and Shandong Provincial Key Medical and Health Discipline of Oral Medicine (2024–2026).

Appendix A. Supplementary data

Supplementary data to this article can be found online at https://doi.org/10.1016/j.heliyon.2024.e32686.

References

[1] D.F. Kinane, P.G. Stathopoulou, P.N. Papapanou, Periodontal diseases, Nat. Rev. Dis. Prim. 3 (2017) 17038, https://doi.org/10.1038/nrdp.2017.38.

[2] G. Collaborators, Global, regional, and national incidence, prevalence, and years lived with disability for 354 diseases and injuries for 195 countries and territories, 1990-2017: a systematic analysis for the Global Burden of Disease Study 2017, Lancet (London, England) (2018), https://doi.org/10.1016/S0140-6736(18)32279-7.

[3] N. Kassebaum, E. Bernabé, M. Dahiya, B. Bhandari, C. Murray, W. Marcenes, Global burden of severe periodontitis in 1990-2010: a systematic review and meta-regression, J. Dent. Res. 93 (11) (2014) 1045–1053, https://doi.org/10.1177/0022034514552491.

[4] B.-M. Seo, M. Miura, S. Gronthos, P.M. Bartold, S. Batouli, J. Brahim, M. Young, P.G. Robey, C.Y. Wang, S. Shi, Investigation of multipotent postnatal stem cells from human periodontal ligament, Lancet 364 (9429) (2004) 149–155, https://doi.org/10.1016/S0140-6736(04)16627-0.

[5] C. Manresa, E.C. Sanz-Miralles, J. Twigg, M. Bravo, Supportive periodontal therapy (SPT) for maintaining the dentition in adults treated for periodontitis, Cochrane Database Syst. Rev. (1) (2018), https://doi.org/10.1002/14651858.CD009376.pub2.

[6] J. Slots, Periodontitis: facts, fallacies and the future, Periodontology 75 (1) (2017) 7–23, https://doi.org/10.1111/prd.12221.

[7] M. Shimono, T. Ishikawa, H. Ishikawa, H. Matsuzaki, S. Hashimoto, T. Muramatsu, K. Shima, K.I. Matsuzaka, T. Inoue, Regulatory mechanisms of periodontal regeneration, Microsc. Res. Tech. 60 (5) (2003) 491–502, https://doi.org/10.1002/jemt.10290.

[8] W. Beertsen, C.A. McCulloch, J. Sodek, The periodontal ligament: a unique, multifunctional connective tissue, Periodontology 13 (1) (1997) 20–40, https://doi.org/10.1111/j.1600-0757.1997.tb00094.x.

[9] F.-M. Chen, L.-N. Gao, B.-M. Tian, X.-Y. Zhang, Y.-J. Zhang, G.-Y. Dong, H. Lu, Q. Chu, J. Xu, Y.J.S.c.r. Yu, therapy, Treatment of periodontal intrabony defects using autologous periodontal ligament stem cells: a randomized clinical trial, Stem Cell Res. Ther. 7 (2016) 1–11, https://doi.org/10.1186/s13287-016-0288-1.

[10] P. Bartold, S. Gronthos, S. Ivanovski, A. Fisher, D. Hutmacher, Tissue engineered periodontal products, J. Periodontal. Res. 51 (1) (2016) 1–15, https://doi.org/10.1111/jre.12275.

[11] G. Ding, Y. Liu, W. Wang, F. Wei, D. Liu, Z. Fan, Y. An, C. Zhang, S. Wang, Allogeneic periodontal ligament stem cell therapy for periodontitis in swine, Stem cells 28 (10) (2010) 1829–1838, https://doi.org/10.1002/stem.512.

[12] L. Du, R. Feng, S. Ge, PTH/SDF-1α cotherapy promotes proliferation, migration and osteogenic differentiation of human periodontal ligament stem cells, Cell Prolif. 49 (5) (2016) 599–608, https://doi.org/10.1111/cpr.12286.

[13] S. Liu, Y.-N. Wang, B. Ma, J. Shao, H. Liu, S. Ge, Interfaces, Gingipain-responsive thermosensitive hydrogel loaded with SDF-1 facilitates in situ periodontal tissue regeneration, ACS Applied Materials 13 (31) (2021) 36880–36893, https://doi.org/10.1021/acsami.1c08855.

[14] H. Liu, M. Li, L. Du, P. Yang, S. Ge, E. C, Local administration of stromal cell-derived factor-1 promotes stem cell recruitment and bone regeneration in a rat periodontal bone defect model, Mater. Sci. 53 (2015) 83–94, https://doi.org/10.1016/j.msec.2015.04.002.

[15] K. Higashino, M. Viggeswarapu, M. Bargouti, H. Liu, L. Titus, S.D. Boden, Stromal cell-derived factor-1 potentiates bone morphogenetic protein-2 induced bone formation, Tissue Eng. 17 (3–4) (2011) 523–530, https://doi.org/10.1089/ten.tea.2010.0168.

[16] A. Cipitria, K. Boettcher, S. Schoenhals, D.S. Garske, K. Schmidt-Bleek, A. Ellinghaus, A. Dienelt, A. Peters, M. Mehta, C.M. Madl, In-situ tissue regeneration through SDF-1α driven cell recruitment and stiffness-mediated bone regeneration in a critical-sized segmental femoral defect, Acta Biomater. 60 (2017) 50–63, https://doi.org/10.1016/j.actbio.2017.07.032.

[17] Q. Liang, L. Du, R. Zhang, W. Kang, S. Ge, Stromal cell-derived factor-1/Exendin-4 cotherapy facilitates the proliferation, migration and osteogenic differentiation of human periodontal ligament stem cells in vitro and promotes periodontal bone regeneration in vivo, Cell Prolif. 54 (3) (2021) e12997, https://doi.org/10.1111/cpr.12997.

[18] A. Thakur, R. Sharma, V.S. Jaswal, E. Nepovimova, A. Chaudhary, K. Kuca, Psoralen: a biologically important coumarin with emerging applications, Mini Rev. Med. Chem. 20 (18) (2020) 1838–1845, https://doi.org/10.2174/1389557520666200429101053.

[19] H. Li, J. Xu, X. Li, Y. Hu, Y. Liao, W. Zhou, Z. Song, Anti-inflammatory activity of psoralen in human periodontal ligament cells via estrogen receptor signaling pathway, Sci. Rep. 11 (1) (2021) 8754, https://doi.org/10.1038/s41598-021-85145-1.

[20] T. Zhang, W. Han, K. Zhao, W. Yang, X. Lu, Y. Jia, A. Qin, Y. Qian, Psoralen accelerates bone fracture healing by activating both osteoclasts and osteoblasts, Faseb. J. 33 (4) (2019) 5399–5410, https://doi.org/10.1096/fj.201801797R.

[21] L. Ge, K. Cheng, J. Han, A network pharmacology approach for uncovering the osteogenic mechanisms of Psoralea corylifolia Linn, Evid. base Compl. Alternative Med. : eCAM 2019 (2019), https://doi.org/10.1155/2019/2160175.

[22] Y. Huang, L. Liao, H. Su, X. Chen, T. Jiang, J. Liu, Q. Hou, Psoralen accelerates osteogenic differentiation of human bone marrow mesenchymal stem cells by activating the TGF-β/Smad3 pathway, Exp. Ther. Med. 22 (3) (2021) 1–9, https://doi.org/10.3892/etm.2021.10372.

[23] B.-F. Yin, Z.-L. Li, Z.-Q. Yan, Z. Guo, J.-W. Liang, Q. Wang, Z.-D. Zhao, P.-L. Li, R.-C. Hao, M.-Y. Han, Correction to: psoralen alleviates radiation-induced bone injury by rescuing skeletal stem cell stemness through AKT mediated up-regulation of GSK-3β and NRF2, Stem Cell Res. Ther. 13 (1) (2022) 361, https://doi.org/10.1186/s13287-022-02911-2.

[24] X. Li, C. Yu, Y. Hu, X. Xia, Y. Liao, J. Zhang, H. Chen, W. Lu, W. Zhou, Z. Song, New application of psoralen and angelicin on periodontitis with anti-bacterial, anti-inflammatory, and osteogenesis effects, Front. Cell. Infect. Microbiol. 8 (2018) 178, https://doi.org/10.3389/fcimb.2018.00178.

[25] H. Liu, Y. Xu, Q. Cui, N. Liu, F. Chu, B. Cong, Y. Wu, Effect of psoralen on the intestinal barrier and alveolar bone loss in rats with chronic periodontitis, Inflammation 44 (2021) 1843–1855, https://doi.org/10.1007/s10753-021-01462-7.

[26] Y. Liang, X. Luan, X. Liu, Recent advances in periodontal regeneration: a biomaterial perspective, Bioact. Mater. 5 (2) (2020) 297–308, https://doi.org/10.1016/j.bioactmat.2020.02.012.

[27] Y. Wei, Y. Deng, S. Ma, M. Ran, Y. Jia, J. Meng, F. Han, J. Gou, T. Yin, H. He, Local drug delivery systems as therapeutic strategies against periodontitis: a systematic review, J. Contr. Release 333 (2021) 269–282, https://doi.org/10.1016/j.jconrel.2021.03.041.

[28] M. Grundmann-Kollmann, M. Podda, L. Bräutigam, K. Hardt-Weinelt, R.J. Ludwig, G. Geisslinger, R. Kaufmann, I.J.B.j.o.c.p. Tegeder, Spatial distribution of 8-methoxypsoralen penetration into human skin after systemic or topical administration, Br. J. Clin. Pharmacol. 54 (5) (2002) 535–539, https://doi.org/10.1046/j.1365-2125.2002.01692.x.

[29] D.N. Heo, W.-K. Ko, M.S. Bae, J.B. Lee, D.-W. Lee, W. Byun, C.H. Lee, E.-C. Kim, B.-Y. Jung, I.K. Kwon, Enhanced bone regeneration with a gold nanoparticle–hydrogel complex, J. Mater. Chem. B 2 (11) (2014) 1584–1593, https://doi.org/10.1039/c3tb21246g.

[30] K. Yue, G. Trujillo-de Santiago, M.M. Alvarez, A. Tamayol, N. Annabi, A. Khademhosseini, Synthesis, properties, and biomedical applications of gelatin methacryloyl (GelMA) hydrogels, Biomaterials 73 (2015) 254–271, https://doi.org/10.1016/j.biomaterials.2015.08.045.

[31] Z. Yuan, X. Yuan, Y. Zhao, Q. Cai, Y. Wang, R. Luo, S. Yu, Y. Wang, J. Han, L. Ge, Injectable GelMA cryogel microspheres for modularized cell delivery and potential vascularized bone regeneration, Small 17 (11) (2021) 2006596, https://doi.org/10.1002/smll.202006596.

[32] Y.-H. Kim, J.I. Dawson, R.O. Oreffo, Y. Tabata, D. Kumar, C. Aparicio, I. Mutreja, Gelatin methacryloyl hydrogels for musculoskeletal tissue regeneration, Bioengineering 9 (7) (2022) 332, https://doi.org/10.3390/bioengineering9070332.

[33] M. Vigata, C.D. O'connell, S. Cometta, D.W. Hutmacher, C. Meinert, N. Bock, Gelatin methacryloyl hydrogels for the localized delivery of cefazolin, Polymers 13 (22) (2021) 3960, https://doi.org/10.3390/polym13223960.

[34] Y. Zhang, Z. Wang, Q. Hu, H. Luo, B. Lu, Y. Gao, Z. Qiao, Y. Zhou, Y. Fang, J. Gu, 3D bioprinted GelMA-nanoclay hydrogels induce colorectal cancer stem cells through activating wnt/β-catenin signaling, Small 18 (18) (2022) 2200364, https://doi.org/10.1002/smll.202200364.

[35] R. Goto, E. Nishida, S. Kobayashi, M. Aino, T. Ohno, Y. Iwamura, T. Kikuchi, J.-i. Hayashi, G. Yamamoto, M. Asakura, Gelatin methacryloyl–riboflavin (Gelma–rf) hydrogels for bone regeneration, Int. J. Mol. Sci. 22 (4) (2021) 1635, https://doi.org/10.3390/ijms22041635.

[36] G. Jiang, S. Li, K. Yu, B. He, J. Hong, T. Xu, J. Meng, C. Ye, Y. Chen, Z. Shi, A 3D-printed PRP-GelMA hydrogel promotes osteochondral regeneration through M2 macrophage polarization in a rabbit model, Acta Biomater. 128 (2021) 150–162, https://doi.org/10.1016/j.actbio.2021.04.010.

[37] T. Kaneda, M. Miyauchi, T. Takekoshi, S. Kitagawa, M. Kitagawa, H. Shiba, H. Kurihara, T. Takata, Characteristics of periodontal ligament subpopulations obtained by sequential enzymatic digestion of rat molar periodontal ligament, Bone 38 (3) (2006) 420–426, https://doi.org/10.1016/j.bone.2005.08.021.

[38] J. Yu, X. Wu, W. Zhang, F. Chu, Q. Zhang, M. Gao, Y. Xu, Y. Wu, Effect of psoralen on the regulation of osteogenic differentiation induced by periodontal stem cell-derived exosomes, Hum. Cell (2023) 1–14, https://doi.org/10.1007/s13577-023-00918-2.

[39] Z. Yang, X.W. Zhang, F.F. Zhuo, T.T. Liu, Q.W. Luo, Y.Z. Zheng, L. Li, H. Yang, Y.C. Zhang, Y.H. Wang, Allosteric activation of transglutaminase 2 via inducing an "open" conformation for osteoblast differentiation, Adv. Sci. (2023) 2206533, https://doi.org/10.1002/advs.202206533.
[40] X.-Q. Li, X. Du, D.-M. Li, P.-Z. Kong, Y. Sun, P.-F. Liu, Q.-S. Wang, Y.-M. Feng, ITGBL1 is a Runx2 transcriptional target and promotes breast cancer bone metastasis by activating the TGFβ signaling pathway, Cancer Res. 75 (16) (2015) 3302–3313, https://doi.org/10.1158/0008-5472.CAN-15-0240.
[41] X. Wu, T. Zhang, B. Hoff, S. Suvarnapathaki, D. Lantigua, C. McCarthy, B. Wu, G. Camci-Unal, Mineralized hydrogels induce bone regeneration in critical size cranial defects, Adv. Healthcare Mater. 10 (4) (2021) 2001101, https://doi.org/10.1002/adhm.202001101.